

# Supporting Information

## Decoupling the Geometric Parameters of Shape- Controlled Pd Nanocatalysts

*Moitree Laskar and Sara E. Skrabalak\**

Department of Chemistry, Indiana University, 800 E Kirkwood Ave. Bloomington, IN-47405

(United States)

\*Corresponding Author. E-mail: [sskrabal@indiana.edu](mailto:sskrabal@indiana.edu)

## Discussion on Nanocrystal Size Optimization

The size of the Pd nanocubes was controlled by two methods: (i) varying the amount of seed solution<sup>1,2</sup> and (ii) varying the amount of Pd precursor, keeping all other parameters constant. Varying the volume of seed solution produces nanocubes with edge lengths varying from 35-56 nm. A larger volume of seed solution yielded nanocubes with smaller edge lengths. Nanocubes with edge lengths smaller than 35 nm can be achieved by reducing the amount of Pd precursor. As expected, a smaller amount of Pd precursor generates smaller Pd nanocubes. SEM and TEM images in Figure 1 clearly indicate that size-controlled synthesis is achieved by the seeded-growth method. The well-defined cubic shape of the seed acted as a template to influence the final shape of the crystals.

Pd octahedra of average edge length 23 nm were prepared following a reported method by reducing potassium tetrachloropalladate ( $K_2PdCl_4$ ) by L-ascorbic acid (AA) and citric acid in an aqueous solution containing cetyltrimethylammonium chloride (CTAC).<sup>3</sup> An SEM image of Pd octahedra having an edge length of 23 nm is shown in Figure 2a, and their TEM images and size distributions are provided in the inset. These Pd nanooctahedra were used as seeds for the formation of size-controlled Pd nanooctahedra.

Unfortunately, reproducibly controlling the size of Pd nanooctahedra according to the reported literature method was not possible.<sup>2</sup> Inspired by the seed-mediated growth approach described for the synthesis of size controlled Pd nanocubes, a new method was developed for controlling the size of octahedra. Pd nanooctahedra with an average edge length of 26 nm, 32 nm, 37 nm and 48 nm were prepared by reducing  $K_2PdCl_4$  by citric acid in an aqueous solution containing CTAC and octahedral Pd nanoseeds. The size of the nanooctahedra can be controlled

by varying the concentration of the stabilizing agent CTAC. Without a sufficient amount of CTAC, this method produces polydisperse particles with ill-defined shapes. However, a CTAC: Pd ratio of 100:1 and above resulted in well-defined Pd nanooctahedra with high size monodispersity. Shown in Figure 2b-d are the SEM images of Pd nanooctahedra where size of the particles has been gradually increased by decreasing the concentration of CTAC. At low concentration of CTAC the shape of the particles is not stabilized until a threshold limit is reached. Thereafter, a higher concentration of surfactant provides a complete coating of smaller octahedra thereby inhibiting their further growth. However, this method does not produce any Pd nanooctahedra of edge length larger than 37 nm. So, 48 nm Pd (Figure 2e) nanooctahedra were obtained by increasing the amount of Pd precursor keeping all other conditions same as the one which produces 37 nm nanooctahedra. The synthetic procedure developed herein, both the citrate ion and CTAC played important role in stabilizing {111} facet leading to the formation of Pd nanooctahedra.

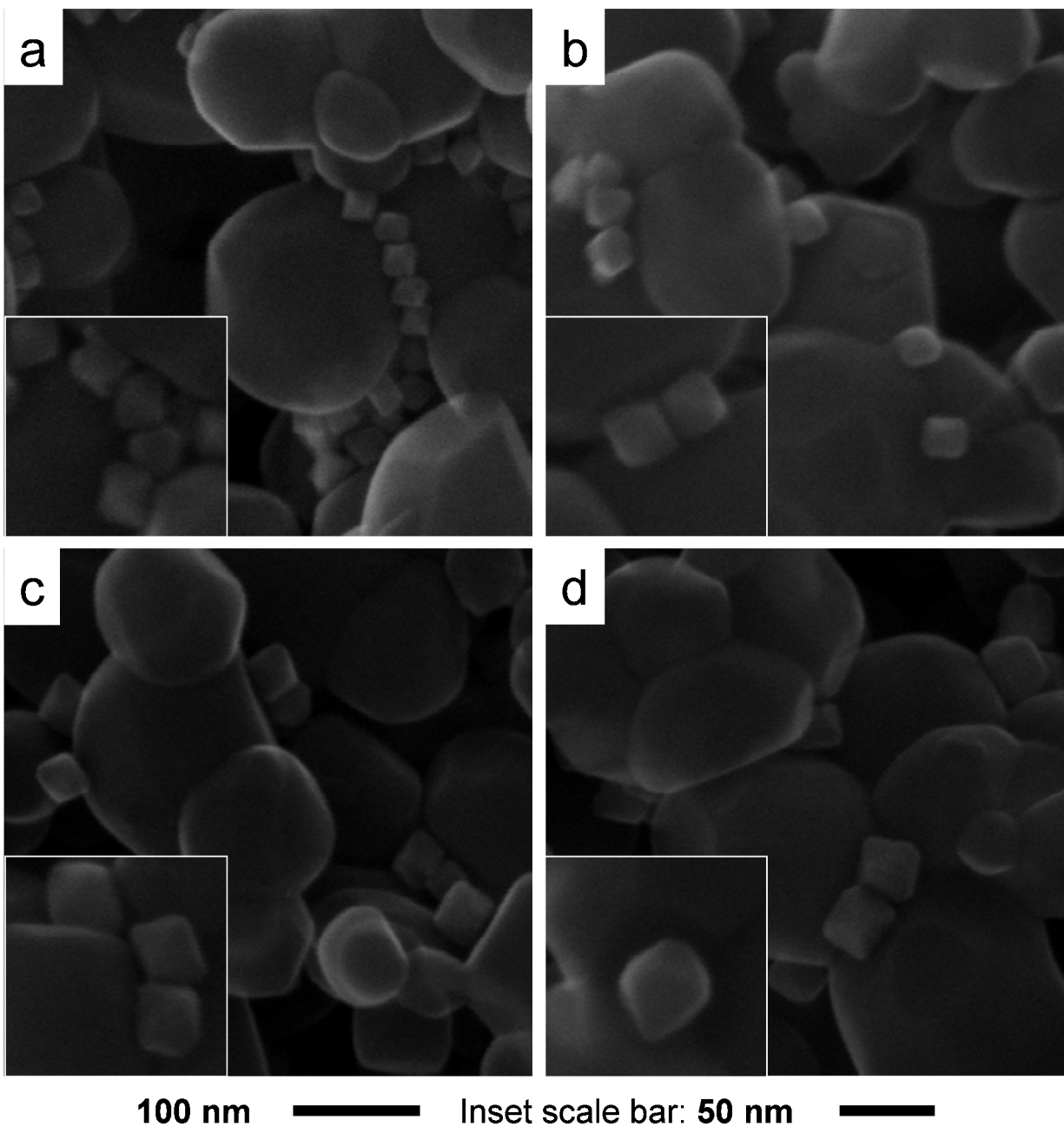


**Figure S1.** SEM images of TiO<sub>2</sub> supported Pd octahedra of edge length (a) 26 nm (b) 32 nm (c) 37 nm and (d) 48 nm before catalytic reaction. Inset: SEM images of the respective sample after use as a hydrogenation catalyst.

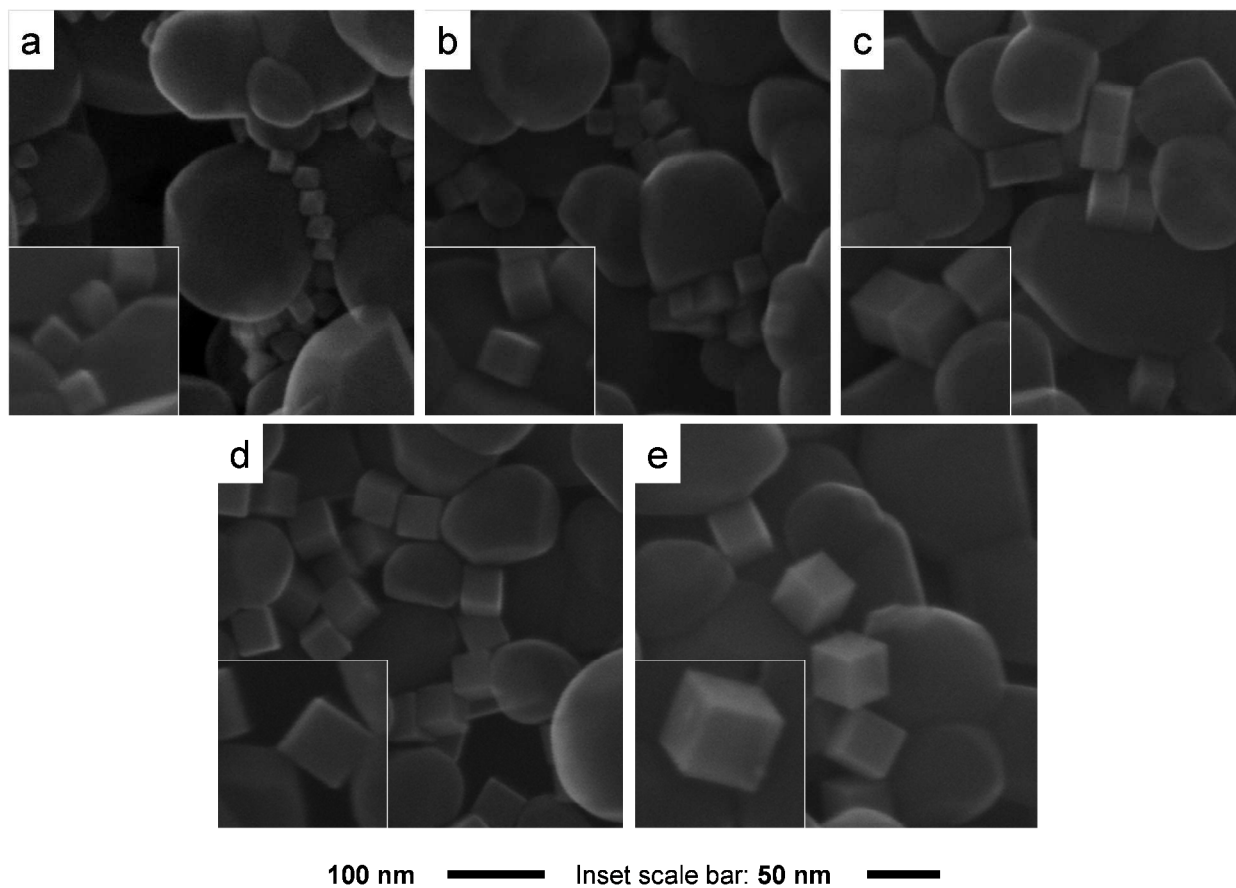


**Figure S2.** SEM images of TiO<sub>2</sub> supported Pd nanocubes of edge length (a) 25 nm (b) 30 nm (c) 35 nm (d) 42 nm and (e) 56 nm before catalytic reaction. Inset: SEM images of the respective sample after use as a hydrogenation catalyst.

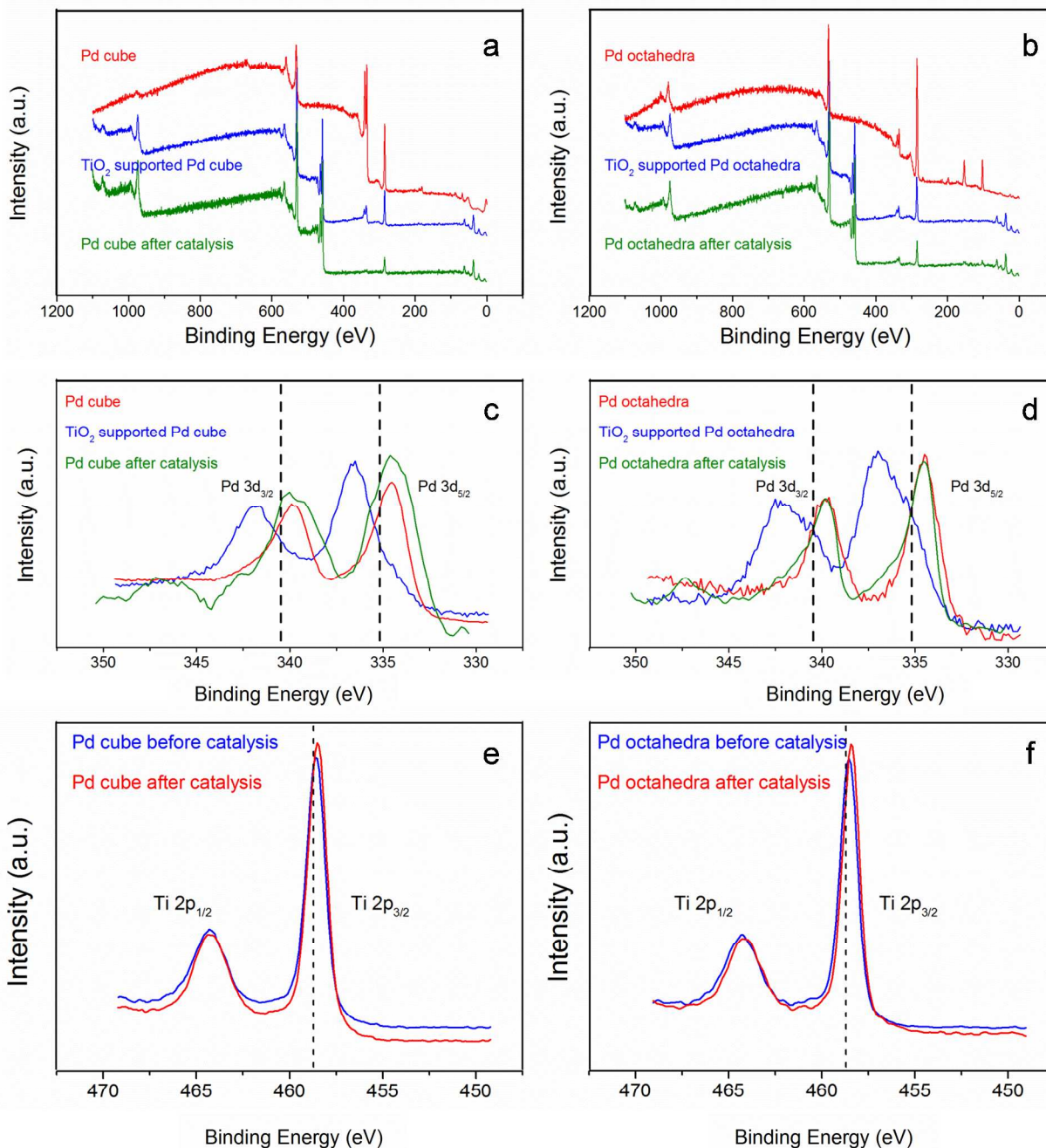


**Figure S3.** XPS (a, b) survey scans and (c, d) Pd 3d region and (e, f) Ti 2p region for (a, c, e) Pd nanocubes (as prepared, TiO<sub>2</sub> supported, and after use) and (b, d, f) Pd octahedral (as prepared, TiO<sub>2</sub> supported, and after use). The dotted lines in (b) and (d) correspond to the binding energy for bulk Pd and in (e) and (f) correspond to the binding energy for Ti in TiO<sub>2</sub>.

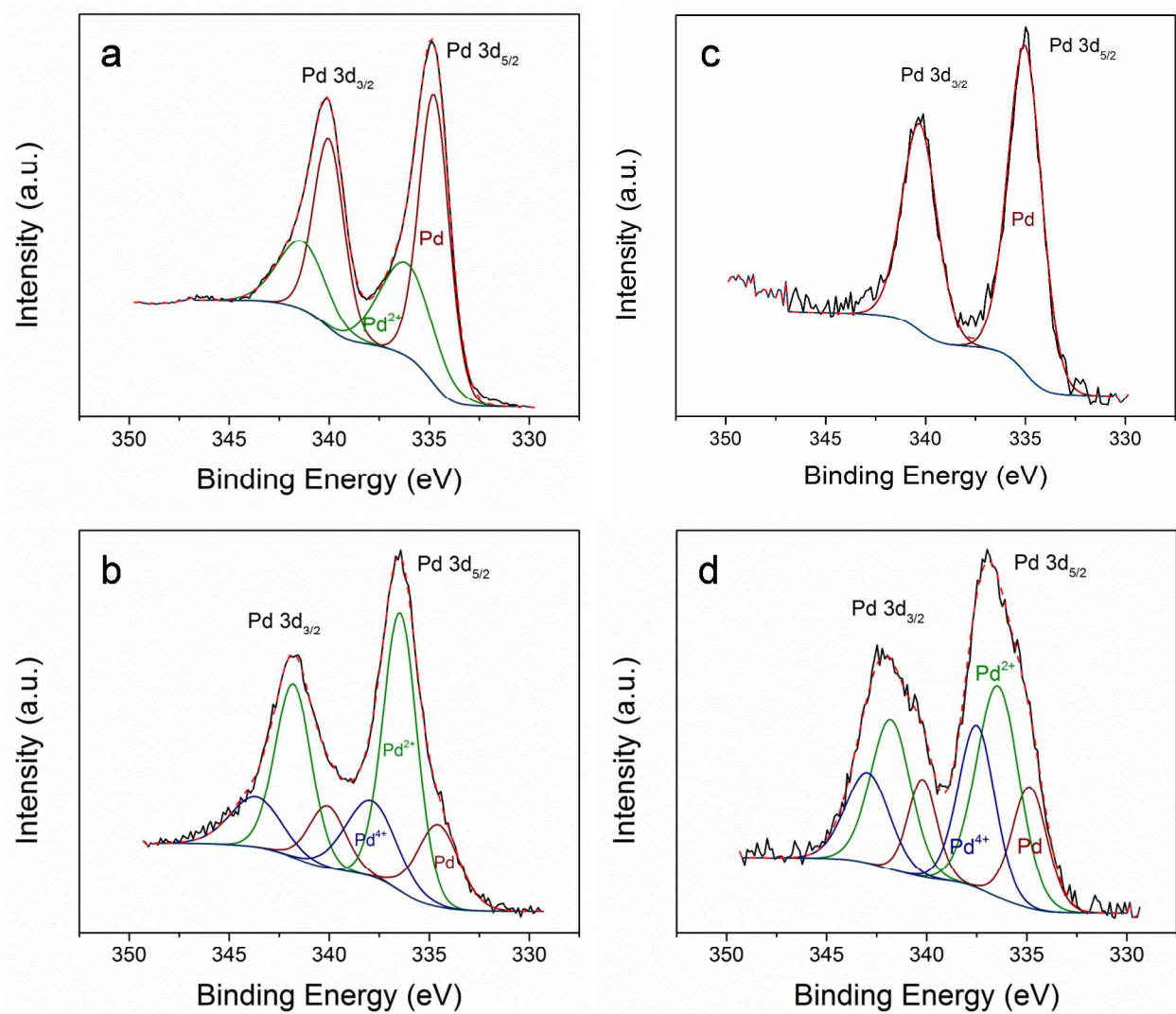


**Figure S4.** XPS deconvolution of Pd 3d<sub>3/2</sub> and 3d<sub>5/2</sub> region for (a) Pd nanocubes, (b) TiO<sub>2</sub> supported Pd nanocubes, (c) Pd nanoctahedra, and (d) TiO<sub>2</sub> supported Pd nanoctahedra.

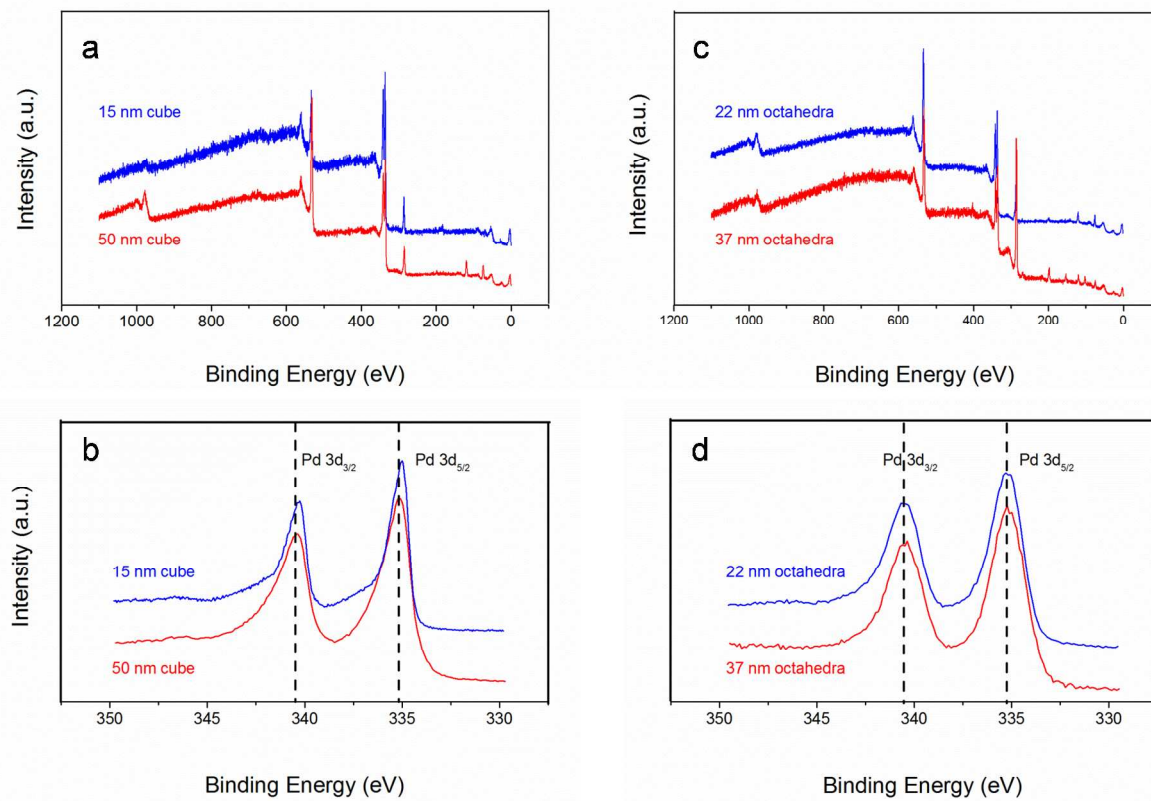


**Figure S5.** XPS (a, c) survey scans and (b, d) Pd 3d region for (a, b) 15 nm and 50 nm unsupported Pd nanocubes and (c, d) 22 nm and 37 nm unsupported Pd nanooctahedra. The dotted lines in (b) and (d) correspond to the binding energy for bulk Pd.

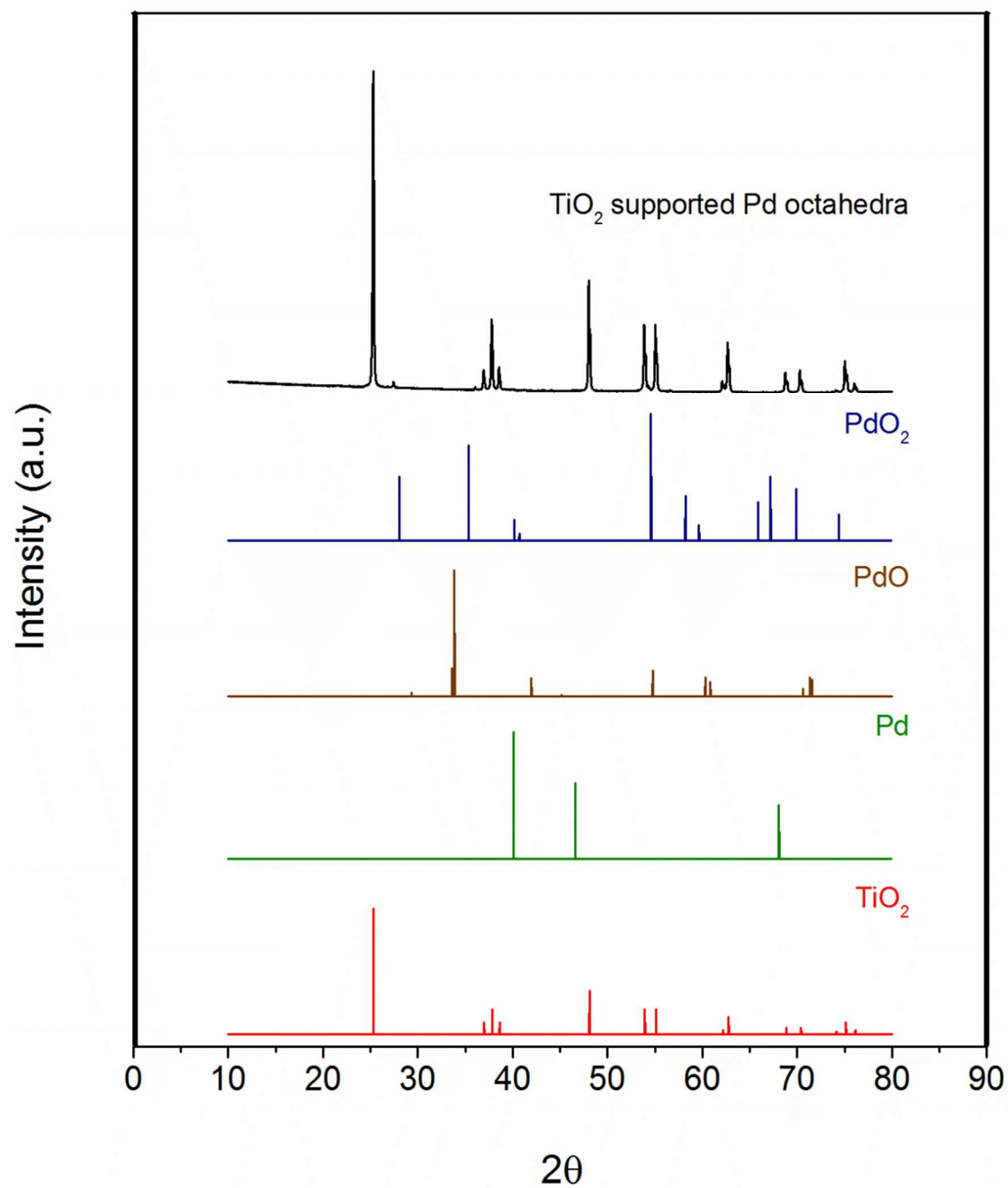


**Figure S6.** Powder X-ray diffraction of pattern of TiO<sub>2</sub> supported Pd octahedra and reference PdO<sub>2</sub> (00-034-1101), PdO (00-041-1107), Pd (00-046-1043), and anatase TiO<sub>2</sub> (00-021-1272).

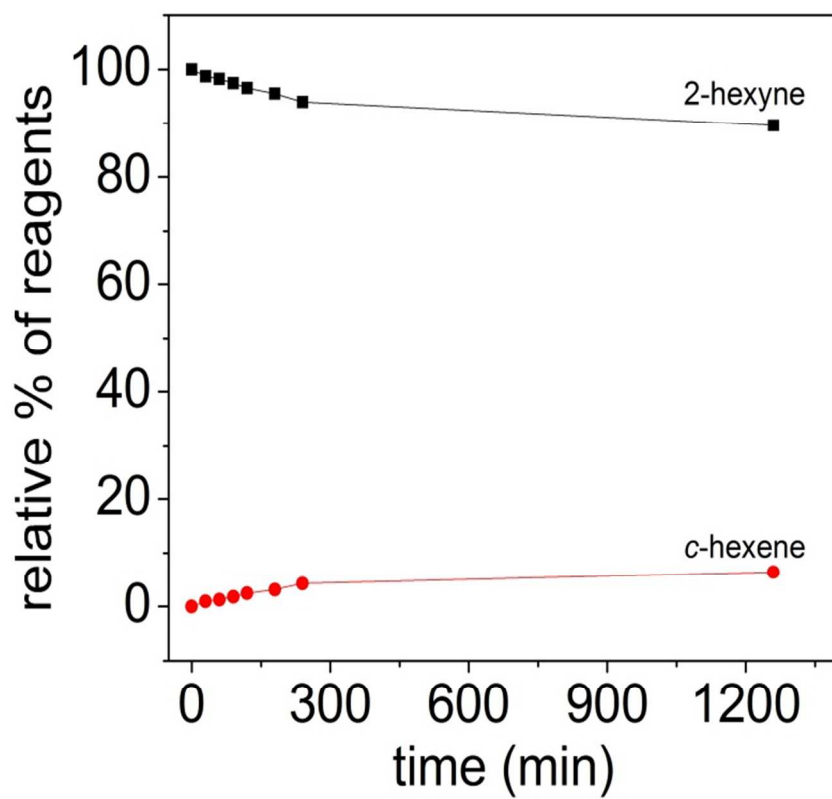
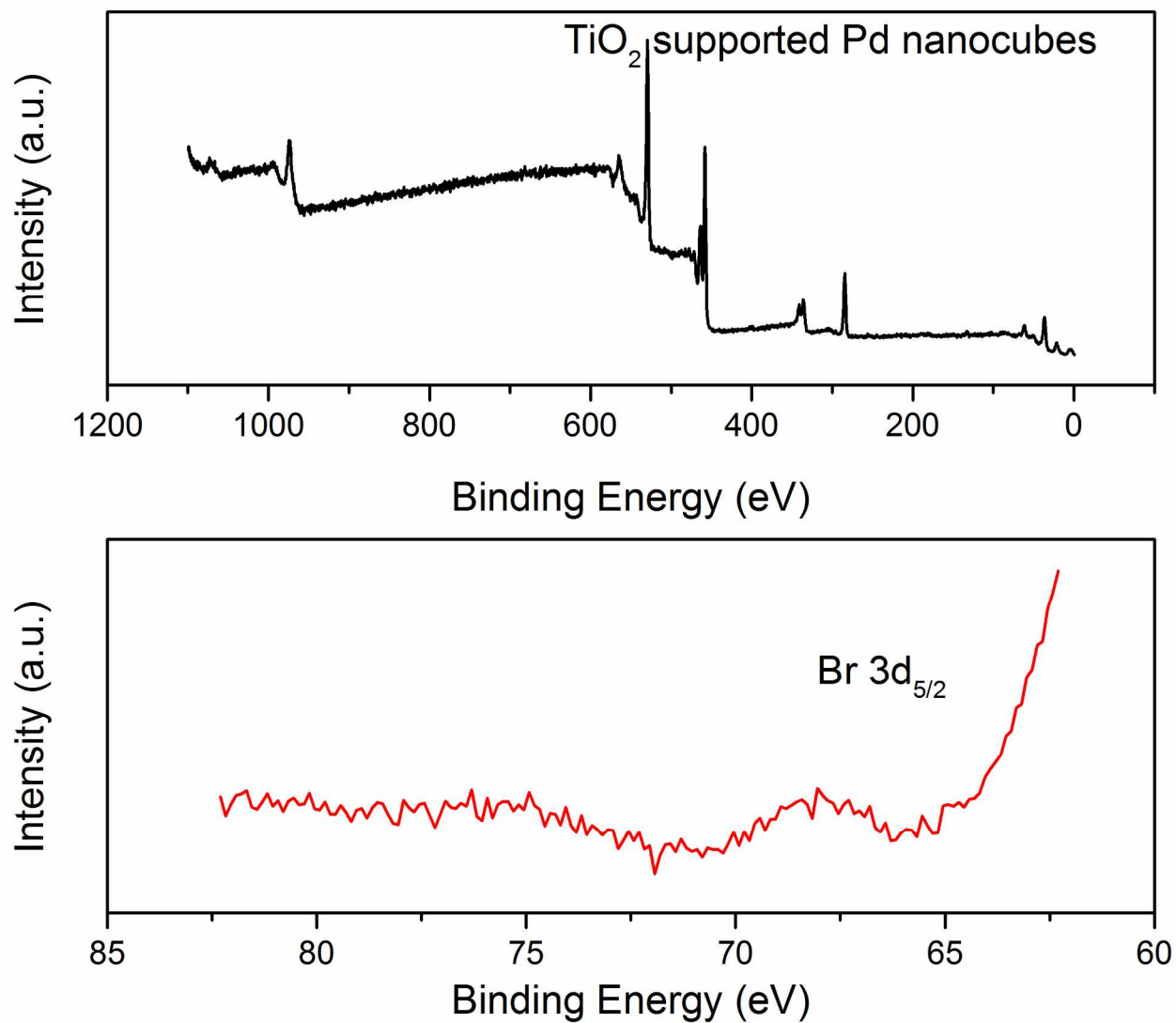
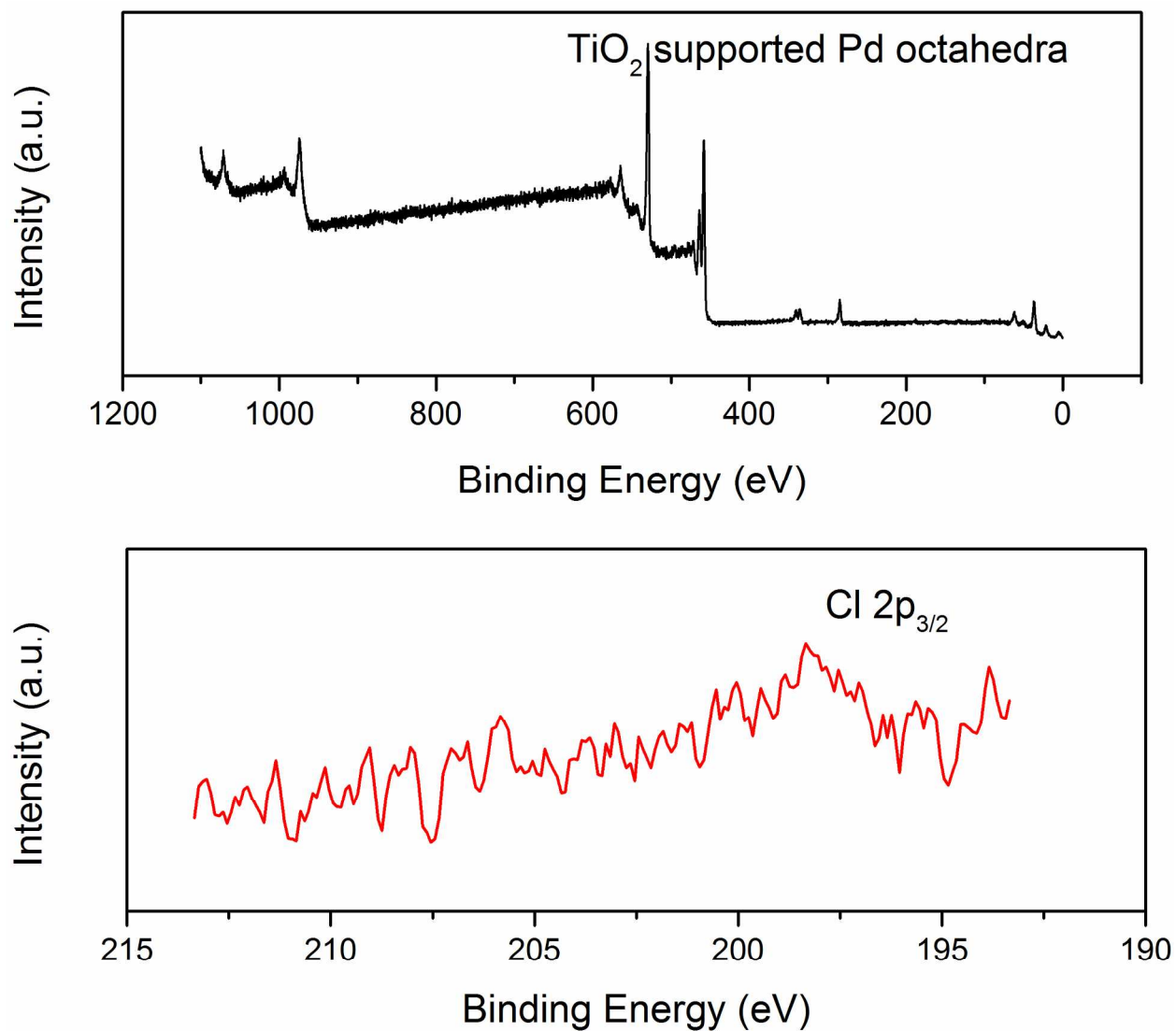


Figure S7. Hydrogenation of 2-hexyne in the presence of TiO<sub>2</sub> only



**Figure S8.** XPS (top) survey scan and (bottom) Br 3d region for a  $\text{TiO}_2$  supported Pd nanocube sample after 100 scans. The binding energy for  $\text{Br}^- 3d_{5/2}$  lies in the region 68-70 eV depending on its environment. The signal-to-noise is poor but assuming a peak, the amount of  $\text{Br}^-$  in this and all other samples was  $<0.1\%$ .



**Figure S9.** XPS (top) survey scan and (bottom) Cl 2p region for a  $\text{TiO}_2$  supported Pd octahedra sample after 100 scans. The binding energy for Cl  $2p_{3/2}$  lies in the region 198-200 eV depending on its environment. The signal-to-noise is poor but assuming a peak, the amount of Cl in this and all other samples was  $\leq 0.3\%$ .

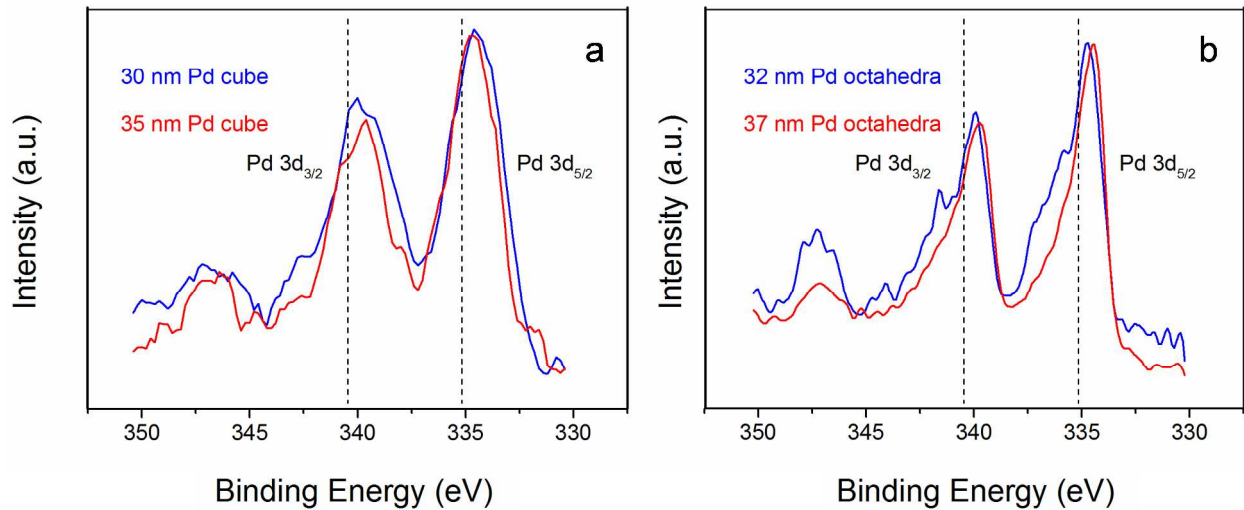


**Figure S10.** XPS (a) Pd 3d region for 30 nm and 35 nm TiO<sub>2</sub> supported Pd nanocubes after catalysis. XPS (b) Pd 3d region for 32 nm and 37 nm TiO<sub>2</sub> supported Pd nanooctahedra after catalysis. The dotted lines correspond to the binding energy for bulk Pd.

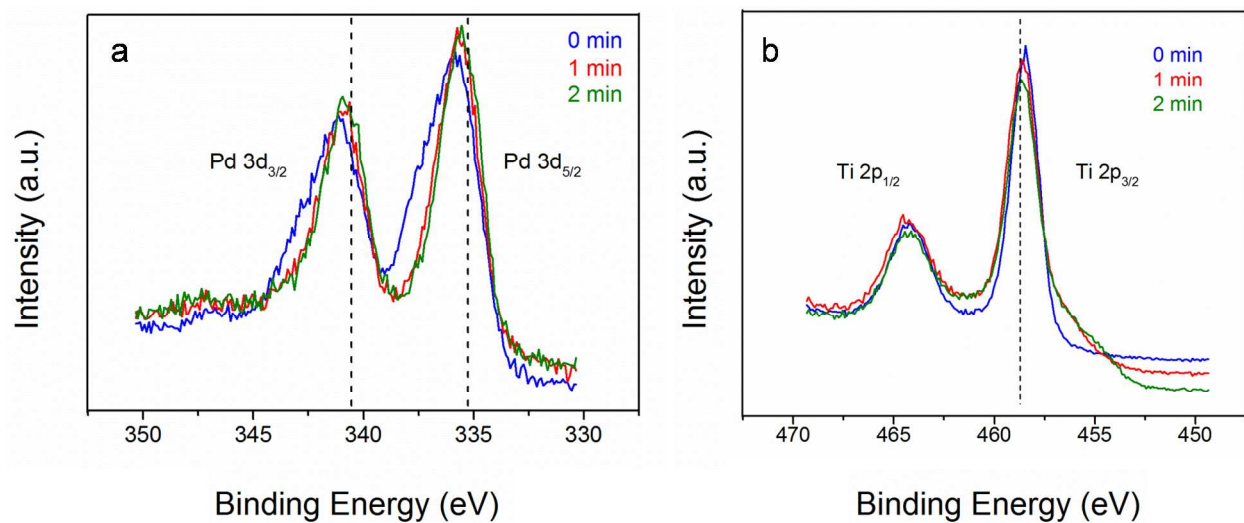


**Figure S11.** XPS (a) Pd 3d region and (b) Ti 2p region for 37 nm TiO<sub>2</sub> supported Pd octahedra after Ar sputtering. The dotted lines correspond to the binding energy for bulk Pd and Ti in TiO<sub>2</sub>.

**Table S1.** Comparison of % of face atoms/ particles and TOF ratio between the smallest and largest Pd nanocubes and nanooctahedra.

Shape	Average Edge Length (nm)	Number of Surface Atoms/ Particle	Number of Face Atoms/ Particle	% of Face Atoms/ Particle	TOF ratio
Pd nanocubes	25	50702	49926	98.47	2.15
	35	99374	98286	98.90	
Pd nanooctahedra	26	36102	34968	96.85	12.06
	48	122502	120408	98.29	

**Table S2.** Average edge lengths, dispersion, face to edge and face to corner atoms ratio of Pd nanocubes and nanoctahedra.

Shape	Average Edge Length (nm)	Dispersion (no. of surface atoms/ no. of total atoms)	Face : Edge Atoms (per particle)	Face : Corner Atoms (per particle)
Pd nanocubes	25	0.04579	64.0	6048.7
	30	0.03821	77.0	8778.7
	35	0.03278	90.0	12015.7
	42	0.02739	108.0	17334.7
	56	0.02061	144.0	30888.7
Pd nanoctahedra	26	0.06120	30.6	5828.0
	32	0.04998	38.0	8893.3
	37	0.04347	44.0	11881.3
	48	0.03370	57.3	20068.0

## REFERENCES

- (1) Niu, W.; Li, Z.-Y.; Shi, L.; Liu, X.; Li, H.; Han, S.; Chen, J.; Xu, G. *Cryst. Growth Des.* **2008**, *8*, 4440.
- (2) Niu, W.; Zhang, L.; Xu, G. *ACS Nano* **2010**, *4*, 1987.
- (3) Hong, J. W.; Kim, D.; Lee, Y. W.; Kim, M.; Kang, S. W.; Han, S. W. *Angew. Chem. Int. Ed.* **2011**, *50*, 8876.